# Characterization of CdTe/CdZnTe detectors

Goro Sato, Tadayuki Takahashi, Masahiko Sugiho, Manabu Kouda,
Takefumi Mitani, Kazuhiro Nakazawa, Yuu Okada and Shin Watanabe

*Abstract*— **In order to characterize CdTe/CdZnTe detectors in a planar configuration, we have developed a new method to extract $\mu\tau$ products. In this method we prepare a analytic spectral model based on the charge transport properties in the device, which is intended to be used in fitting calculation. The low mobility-lifetime ($\mu\tau$) products of carriers in CdTe/CdZnTe detectors produce a position dependency in the charge induction efficiency. The model takes the induction efficiency and interaction positions of photons into account. Since the model is parameterized by $\mu\tau$ products, it can extract $\mu\tau$ products. Here, we demonstrate how the model works based on the results from 2 mm thick HPB CdZnTe and THM CdTe detectors.**

*Keywords*— **Gamma-ray Detector, CdTe, CdZnTe, Spectral modeling, mobility - lifetime products**

## I. Introduction

CADMIUM Telluride (CdTe) and Cadmium Zinc Telluride (CdZnTe, CZT) based detectors have been developed intensively and have recently seen significant improvements [1]. These detectors have high resistivity because of the wide bandgap and also have high photon absorption efficients because of the large atomic number. However, due to the low transport properties of carriers, electron-hole pairs generated in CdTe and CdZnTe detectors by irradiating with $\gamma$-rays cannot be fully collected. This leads to a significant distortion of the spectrum. The mobility-lifetime ($\mu\tau$) products of the carriers are parameters used to describe the characteristics of CdZnTe and CdTe semiconductor detectors [2].

The mobility can be determined by the risetime information of the amplifier when the detector is irradiated by $\alpha$-rays [3]. This method is simple but the obtained values can be affected by the surface condition of the detector, because the mean free path of a $\alpha$-ray in CdTe/CdZnTe is only $\sim$ 10 $\mu$m. Therefore, some attempts have been made to extract transport properties by utilizing the pulse height spectra [4] [5]. These are based on a method to simulate spectra by Monte Carlo calculations including charge transport in the detector. For example, in a method by M. Jung et al. [5], precisely simulated spectra with different sets of parameters are prepared to extract the relation of peak heights for different energy lines and parameters. And then, $\mu_{\rm e}$, $\mu_{\rm h}$ and $\sigma$ (electronic noise) can be determined by comparing the peak heights relation obtained from experimental data with that of the simulation. However, some discrepancies in spectral shape between the experimental data and simulation remain, which are still critical issues for a detector to be used as a spectrometer.

Here, we propose a new method to characterize a CdZnTe/CdTe detector by using the pulse height spectra. The algorithm to construct a spectrum is similar to that proposed by M.Jung et al.. However, we utilize not only the peak height but also the line shape including low energy tail structure taken at different bias voltages to obtain more accurate $\mu\tau$ products of electron and holes for reproducing a spectra. Our method utilizes a spectral model calculated not by Monte Carlo simulation but direct analytic calculation, in order to incorporate the model into the widely used fitting program XSPEC with $\chi^2$ criterion, which is an analysis software for X-ray astronomy [6]. This approach is useful if we need to handle more than 30,000 detectors for characterization [7] [8] and therefore quick response is important. Here, we present the method for modeling the spectra and apply it to CdZnTe/CdTe detectors.

## II. Modeling the CdTe/CdZnTe Spectra

### A. Spectra of CdTe/CdZnTe

In Fig.1 and 2, we show $^{241}$Am and $^{57}$Co spectra obtained by a planar CdZnTe detector grown by the High Pressure Bridgman technique (HPB CZT) (eV products, U.S.) [9]. The dimensions of the detector are 4 mm $\times$ 4 mm $\times$ 2 mm where 2 mm is the thickness of the detector. It is clearly seen that the spectra contain tail structures which extend to the lower pulse height region from a photo-peak of the incident $\gamma$-ray. Part of this "distortion" is attributed to Compton scattering of the $\gamma$-ray in the surrounding materials, but most of it results from the effects of the slow mobility and the short lifetime of carriers, especially for holes. Since the interaction depth becomes deeper for higher energies, the 122 keV $\gamma$-line has a larger tail structure in comparison with the 59.5 keV $\gamma$-line. The peak position and peak counts increase as the bias voltage is increased.

### B. The "$\mu\tau$-model" spectral fitting method

Below 250 keV, photo absorption is the dominant process for $\gamma$-ray interactions in CdTe/CdZnTe. Incident $\gamma$-ray photons are attenuated with an exponential decay

$$N = N_\circ \exp(-\frac{x}{\lambda(E_\gamma)}) \ , \qquad (1)$$

Manuscript received Nov 25, 2001.

G. Sato is with the Institute of Space and Astronautical Science, Sagamihara Kanagawa 229–8510, Japan, and also with Department of Physics, University of Tokyo, Bunkyo, Tokyo, 113–0033, Japan (telephone: 81-42-759-8135, e-mail: gsato@astro.isas.ac.jp)

T. Takahashi, M. Kouda, T. Mitani and S. Watanabe are with the Institute of Space and Astronautical Science, Sagamihara Kanagawa 229–8510, Japan, and also with Department of Physics, University of Tokyo, Bunkyo, Tokyo, 113–0033, Japan.

M. Sugiho and Y. Okada are with Department of Physics, University of Tokyo, Bunkyo, Tokyo, 113–0033, Japan.

K. Nakazawa is with the Institute of Space and Astronautical Science, Sagamihara Kanagawa 229–8510, Japan.

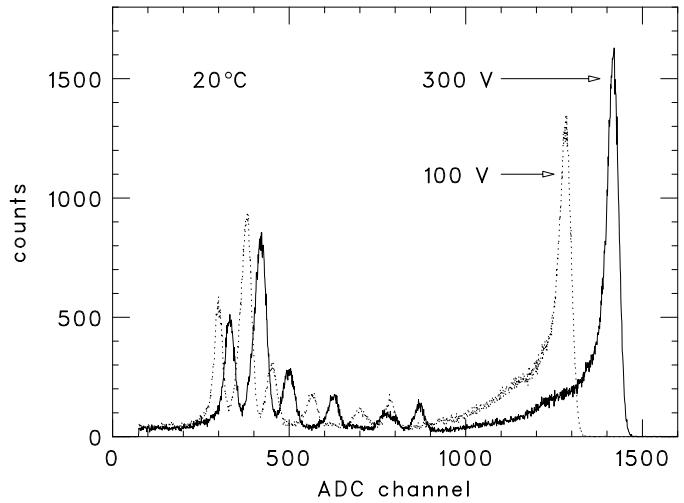


Fig. 1. $^{241}$Am spectra obtained with a 2 mm thick CdZnTe detector. The applied bias voltage is 300 V (solid line) and 100V (dotted line). The operating temperature is 20 °C.

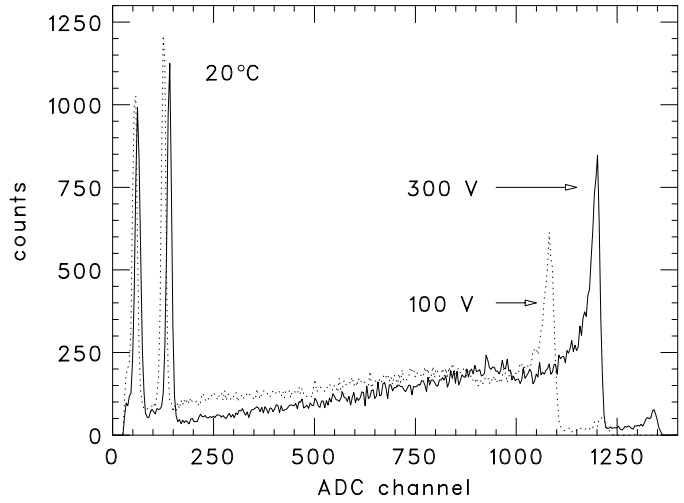


Fig. 2. $^{57}$Co spectra obtained with a 2 mm thick CdZnTe detector. The applied bias voltage is 300 V (solid line) and 100V (dotted line). The operating temperature is 20 °C.

where $x$ is the depth from the irradiated surface and $\lambda$ is the mean free path by photo absorption as a function of energy of the incident $\gamma$-ray. By differentiating Eq.(1), the ratio of photons which interact at the region between $x$ and $x + \mathrm{d}x$ is given as:

$$-\frac{\mathrm{d}N}{N_\circ} = \frac{1}{\lambda(E_\gamma)} \exp(-\frac{x}{\lambda(E_\gamma)})\mathrm{d}x \ . \tag{2}$$

Here, we will assume the ideal situation in which the electric field throughout the detector volume is constant. Then, if we can assume that the detrapping times for both electrons and holes are long and that the gamma rays impinge the negative electrode, the charge induction efficiency is given by the Hecht equation [10]

$$\eta(x) = \frac{\lambda_e}{D}(1 - \exp(-\frac{D-x}{\lambda_e})) + \frac{\lambda_h}{D}(1 - \exp(-\frac{x}{\lambda_h})) \ , \tag{3}$$

TABLE I
PARAMETERS FOR THE "$\mu\tau$-MODEL"

| parameter | content |
|---|---|
| $E_\gamma$ | energy of incident $\gamma$-ray |
| $(\mu\tau)_e$ | $\mu\tau$ product of electron |
| $(\mu\tau)_h$ | $\mu\tau$ product of hole |
| $E$ | strength of electric field |
| $\sigma$ | resolution excluding the tail structure |
| $CH_{\max}$ | channel where Hecht equation becomes unity |

where D is the detector thickness and $\lambda_e$ and $\lambda_h$ are the mean free paths of electrons and holes, respectively, for the case where $\gamma$-rays are irradiated from the cathode face. The mean free paths are related to the $\mu\tau$ products as:

$$\lambda_e = (\mu\tau)_e E, \ \lambda_h = (\mu\tau)_h E \ , \tag{4}$$

where $E$ is the strength of the electric field in the detector. Several papers have shown that quite often in CZT detectors of planar structure, the field distribution is not linear versus depth [11]. However, according to our calculations, the charge collection efficiency does not change significantly when the electric field is bent linearly to the extent that the field extends to full volume of the detector. Then, we calculate with the constant electric field in this paper.

In the calculation, we divide the detector volume into 3000 slices. The detector response for monochromatic $\gamma$-rays is generated by calculating the relative pulse height from Eq.(3) for each slice and summing them by following the weights calculated from Eq.(2). The resultant spectrum gives the shape predicted from the input $\mu\tau$ products. This fitting function (hereafter "$\mu\tau$-model") has parameters as listed in table I.

With the "$\mu\tau$-model" fitting method, we can determine both $(\mu\tau)_e$ and $(\mu\tau)_h$ directly by fitting spectra. In Fig.3, 4 and 5, we present simulated spectra for various sets of parameters. As shown in Fig.3, $(\mu\tau)_e$ is sensitive to the peak channel in a spectrum, while $(\mu\tau)_h$ determines the amount of the tail component, as shown in Fig.4. Since $\lambda$ is the product of $\mu\tau$ and $E$, a change in $E$ affects both $\lambda_e$ and $\lambda_h$ in the same manner. Therefore, a change of the bias voltage also influences the spectral shape in a complex manner, as shown in Fig.5. As the bias voltage increases, the peak channel approaches the limit ($CH_{\max}$) which corresponds to the channel where the efficiency given by the Hecht equation becomes unity, and the amount of the tail structure becomes minimum. Thus, by fitting spectra taken at two different bias voltages (electric fields), we obtain $CH_{\max}$ and $(\mu\tau)_e$. At the same time, the model is fitted to the tail structure by adjusting $(\mu\tau)_h$. The algorithm to construct the fitting function and to fit the model with the data which we have described here is shown in Fig.6.

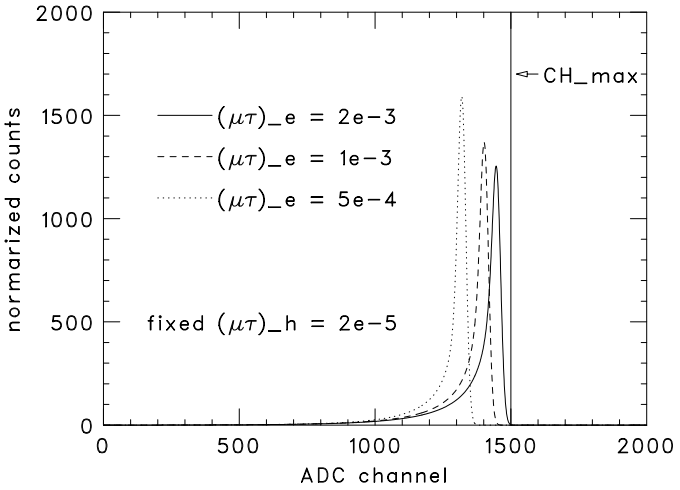


Fig. 3. Model spectra of the 59.5 keV line $\gamma$-rays, with a bias voltage of 300 V and fixed $(\mu\tau)_h$ at $2 \times 10^{-5}$. As $(\mu\tau)_e$ increases, the peak channel goes up.

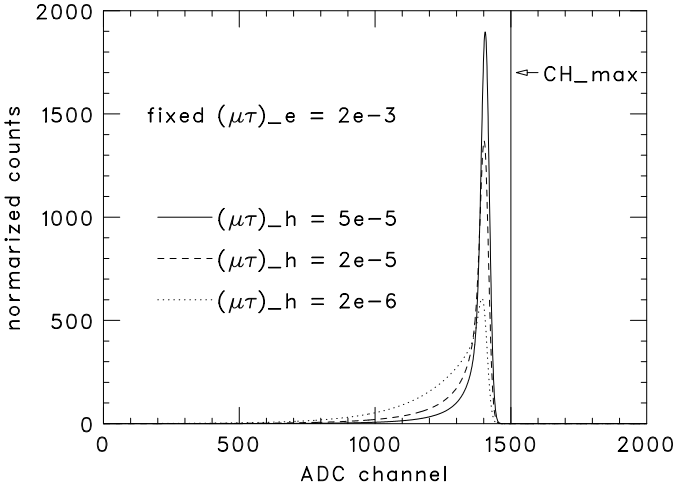


Fig. 4. Model spectra of the 59.5 keV line $\gamma$-rays, with a bias voltage of 300 V and fixed $(\mu\tau)_e$ at $2 \times 10^{-3}$. As $(\mu\tau)_h$ decreases, the tail structure get larger.

### C. Extraction of $\mu\tau$ products

In order to determine $(\mu\tau)_e$ and $(\mu\tau)_h$, at least two spectra taken at different bias voltages are necessary as described above. We obtained spectra at bias voltages of 100 and 300 V using a HPB CdZnTe detector with dimensions of 4 mm $\times$ 4 mm $\times$ 2 mm where 2 mm is the thickness of the detector, which was selected from samples we obtained from eV products. The detector was irradiated with $\gamma$-rays from $^{241}$Am through the cathode face. The signal from the detector is extracted from the anode side and fed into a Charge Sensitive Amplifier (CSA; 5102BS by Clear Pulse, Japan) via a coupling capacitor. The charge signal is integrated in the CSA and shaped by an ORTEC 570 amplifier. With a 1.0 $\mu$sec shaping time, the equivalent RMS noise charge is $\sim$80 electrons at $C_{in}$ = 0 pF and $\sim$270 electrons at $C_{in}$ = 100 pF, respectively. We mounted the detector and the CSA into a thermostatic chamber with the temperature controlled at 20 °C. The leakage current is 1.5 nA and 5 nA for 100 V and 300 V, respectively. The energy resolution (FWHM) of the 59.5 keV peak is 2.1 keV and 1.8 keV.

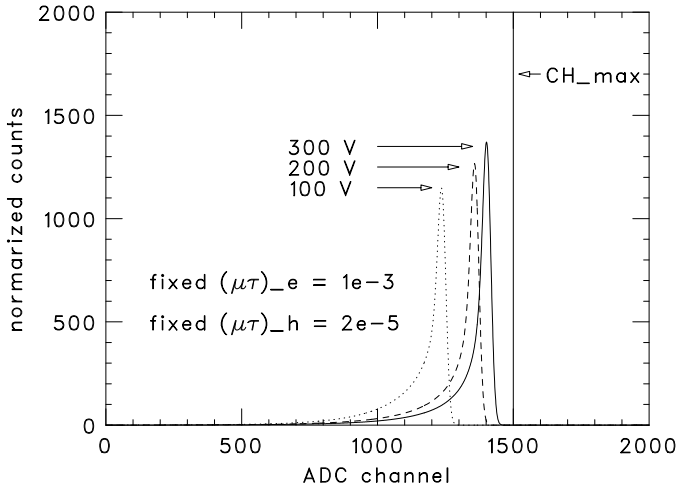


Fig. 5. Model spectra of the 59.5 keV line $\gamma$-rays, with a bias voltage of 300 V (solid line), 200 V (dashes line), and 100 V (dotted line). $\mu\tau$ products are fixed.

We simultaneously fit the spectra obtained with two different bias voltages, 100 V and 300 V, as shown in Fig.7. In the fitting, we properly selected the region to minimize Compton scattering effects because the Compton scattering component from the surrounding materials produces an excess in the lower region of the tail structure. What is more important is the escape peak components. These are the results of photo fluorescence of 23 keV for Cd and 27 keV for Te, which could escape from the detector, especially when it takes place very close to the cathode surface. This effect reduces the channel counts in the photo-peak region. If these escapes are not taken into account, the tail structure is over-estimated, which results in an underestimation of $(\mu\tau)_h$. Therefore, in our method, we use the correction factor for the magnitude of the escape peaks evaluated by Monte Carlo simulations. The correction factor is the ratio of the escape events over photo absorption events. It becomes $\sim$ 9% when 59.5 keV gamma-rays are irradiated on the detector we used for the fitting. By considering the correction, the data were fitted well with the "escape-subtracted $\mu\tau$-model" as shown in Fig.7. The $\mu\tau$ products of CdZnTe detectors were precisely determined to be $1.270\ ^{+0.003}_{-0.001} \times 10^{-3}$ cm$^2$ V$^{-1}$ for electrons and $2.93\ ^{+0.05}_{-0.05} \times 10^{-5}$ cm$^2$ V$^{-1}$ for holes ($\chi^2/\nu = 217/183$). The errors refer to 90% statistical errors. If we ignore the contribution of escapes, $(\mu\tau)_h$ is underestimated to be $2.1 \times 10^{-5}$ cm$^2$ V$^{-1}$. In the following spectral fittings, the amount of events which escape from the main peak is considered when the energy of incident $\gamma$-rays is higher than 23 keV.

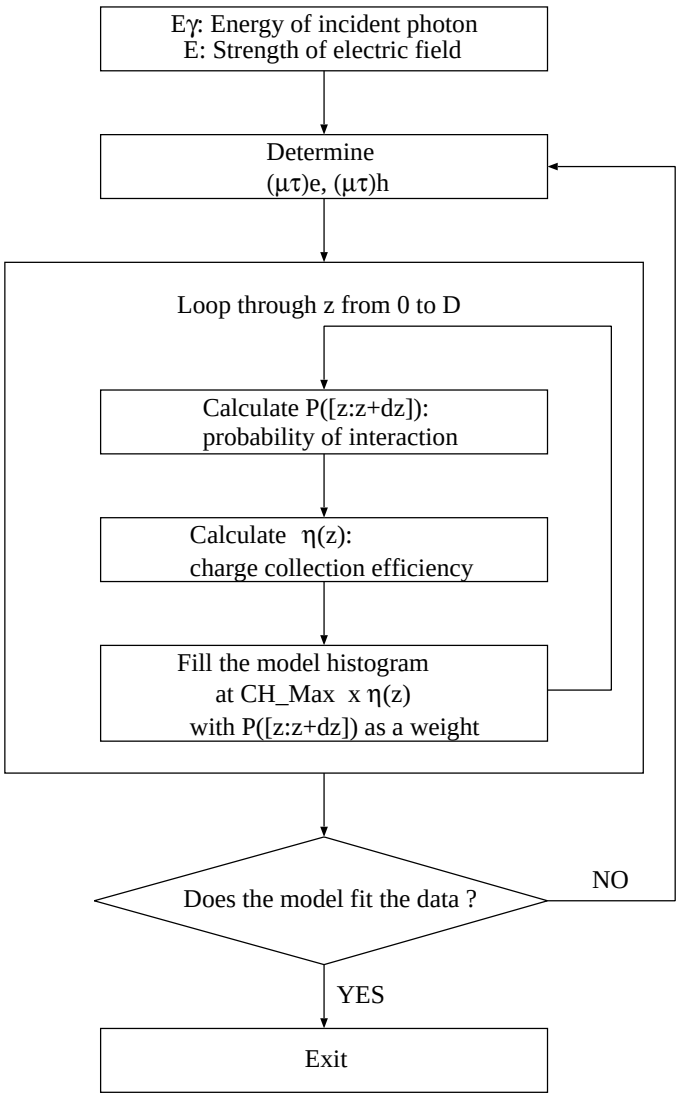


Fig. 6. Algorithm of $\mu\tau$ model

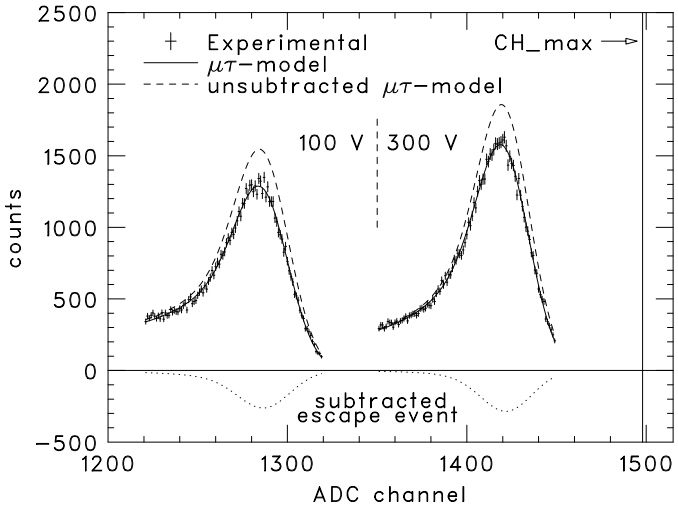


Fig. 7. Fitted spectrum of the 59.5 keV line of $^{241}$Am obtained with a bias voltage of 100 V and 300 V. Fitted model is "$\mu\tau$ model" subtracted by escaping photons. $(\mu\tau)_e$ $(\mu\tau)_h$ are determined as $1.27 \times 10^{-3}$ cm$^2$/V and $2.9 \times 10^{-5}$ cm$^2$/V, respectively.

## III. Verification of $\mu\tau$ products derived from spectral fitting

### A. Fitting for Multiple Energy $\gamma$-ray Spectra

Since $\gamma$-ray lines with different energies have different mean free paths in the detector, the distribution of interaction position changes with energy. Therefore, we derived $\mu\tau$ products from spectra obtained with the same detector used in the previous section by irradiating with various $\gamma$-ray sources (122 keV from $^{57}$Co, 81 keV from $^{133}$Ba, and 22 keV from $^{109}$Cd) in order to make sure that $\mu\tau$ parameters derived from our fitting are valid.

The values of the $\mu\tau$ products obtained from the fitting of multi-energy $\gamma$-rays are summarized in Fig.8 and 9 including the results for the 59.5 keV line in the previous section. Typical statistical errors are 0.2% and 3% for $(\mu\tau)_e$ and $(\mu\tau)_h$, respectively. The $(\mu\tau)_e$ obtained from four different energies are all consistent with each other. On the other hand, while the $(\mu\tau)_h$ obtained for $\gamma$-rays above 59.5 keV show similar values, the one extracted from soft $\gamma$-rays (22 keV from $^{109}$Cd) is lower by a factor of $\sim$3. We will discuss this phenomena in the next section.

### B. Comparison with $\alpha$ particle Method

We now compare the $\mu\tau$ products obtained from our method with those obtained from the $\alpha$ particle measurements performed with the same device at a temperature of 20 °C. We used an $^{241}$Am source emitting 5.5 MeV $\alpha$ particles. The shape of the output pulse of the CSA is recorded with a digital oscilloscope. First, we irradiated the $\alpha$ particles on the cathode surface. In this case, the output signal reflects the movement of the electrons only. Then, to obtain the signal from the holes, we simply reversed the polarity of the bias voltage. From Eq.(3), the pulse height of the output signal depends on the bias voltage and is described as:

$$V_{out} \propto \frac{\mu\tau V_{bias}}{D^2}(1 - \exp(-\frac{D^2}{\mu\tau V_{bias}})). \qquad (5)$$

We applied bias voltages of 10 – 1000 V for electron measurements and of 100 – 1500 V for hole measurements. The obtained pulse heights are plotted in Fig.10. We can fit the data well with the curves predicted from the Eq.(5). The $\mu\tau$ products obtained are shown in Fig.8 and 9.

Compared with the results obtained from four multi-energy $\gamma$-rays, the $\alpha$ measurement shows lower $\mu\tau$ products than the values derived from higher energy $\gamma$-lines (from $^{57}$Co, a $^{133}$Ba, $^{241}$Am) by a factor of 1.3 and 3 for both electrons and holes, respectively.

The geometry of the detector is a key to understand these lower $\mu\tau$ products for the $\alpha$ measurement, as well as the $^{109}$Cd $\gamma$-ray measurement. The mean free path of an $\alpha$-ray is $\sim$10 $\mu$m and that of a 22 keV $\gamma$-ray is $\sim$100 $\mu$m. Therefore, carriers start to move from the region very close to the surface in these cases, and the low value of the $\mu\tau$ products can be explained as an artifact due to the distortion

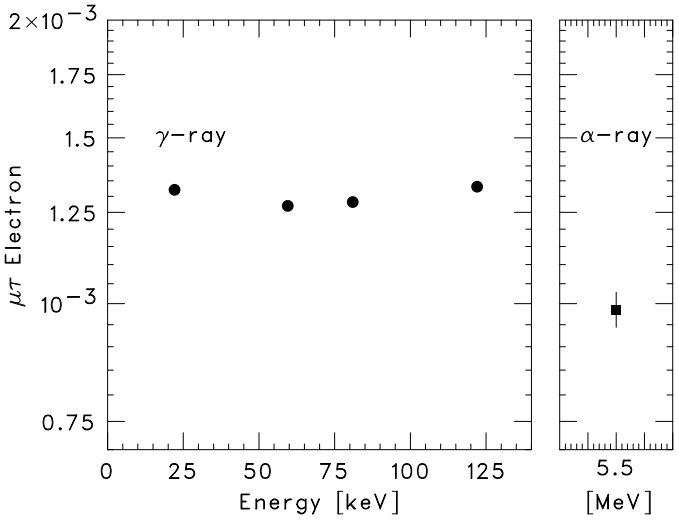


Fig. 8. (*left*) $(\mu\tau)_e$ derived for 22 keV, 59.5 keV, 81 keV and 122.1 keV $\gamma$-rays. (*right*) $(\mu\tau)_e$ measured by $\alpha$-particle method.

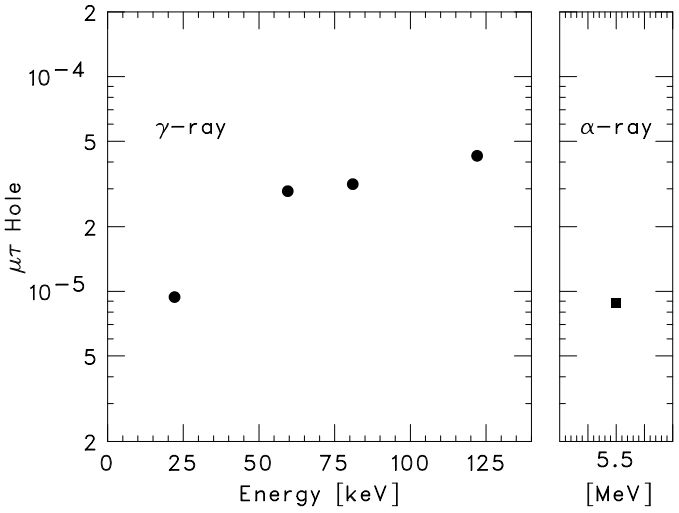


Fig. 9. (*left*) $(\mu\tau)_h$ derived for 22 keV, 59.5 keV, 81 keV and 122.1 keV $\gamma$-lines. (*right*) $(\mu\tau)_h$ measured by $\alpha$-particle method.

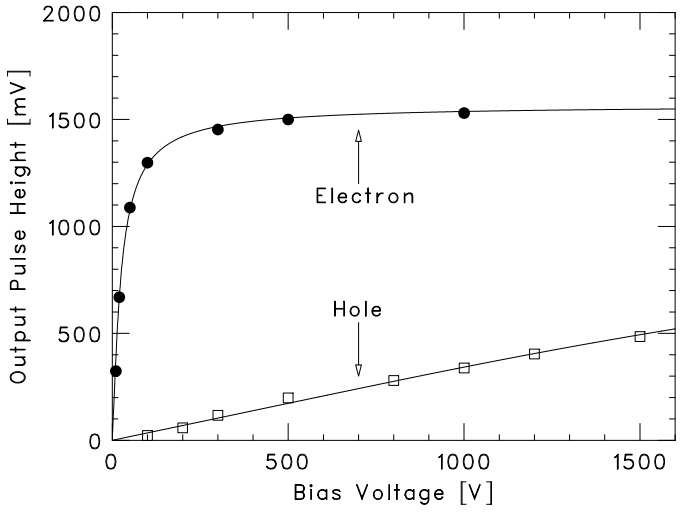


Fig. 10. Obtained output pulse height with a various bias voltages in $\alpha$-ray measurements. The signal from the movement of hole is obtained with a reversed bias voltage. The data are fitted by equation (5) with a $(\mu\tau)_e$ of $9.9 \times 10^{-4}$ cm$^2$/V and a $(\mu\tau)_h$ of $8.8 \times 10^{-6}$ cm$^2$/V.

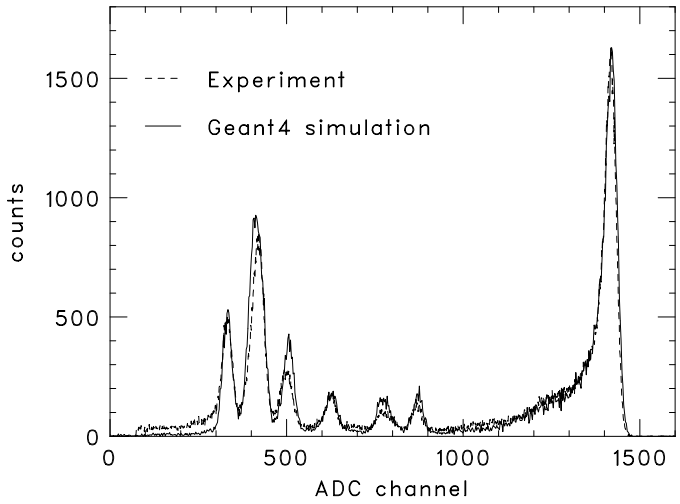


Fig. 11. Simulated spectrum obtained by irradiating $\gamma$-rays from $^{241}$Am, with the experimental measurement.

of the electric field at the surface. It is also important to note that if the mean free path of the holes is significantly shorter than the detector thickness, their movement will be affected by the surface condition much more than the electrons.

For irradiation with higher energy $\gamma$-rays, most of the interactions occur deep inside the device. Therefore, in order to determine the effective $\mu\tau$ products in a detector it is better to consider regions away from the contact (near surface) regions. Here, it would be better to use $\mu\tau$ products extracted by fitting the spectra from the irradiation of the higher energy $\gamma$-rays for the characterization and reconstruction of spectra from CdZnTe and CdTe devices.

### *C. Monte Carlo simulations*

In the spectral fitting with the "$\mu\tau$-model", we intended the effects of escapes and Compton scattering to be minimized. Here, in order to make sure that the treatments work properly, the energy spectrum is simulated by using the Monte Carlo simulator, Geant4 [12]. Geant4 treats electro-magnetic processes such as photo-electric effect, Compton scattering, and ionization. Since secondary generated $\gamma$-rays can be traced by Geant4, the escapes are treated properly. The Compton scattering component from the surrounding materials can be simulated by constructing a mass model. In the simulation, we model the CdZnTe detector with its holder, a source tablet and the thermostatic chamber. In addition to the processes listed above, we incorporate the charge induction efficiency depending

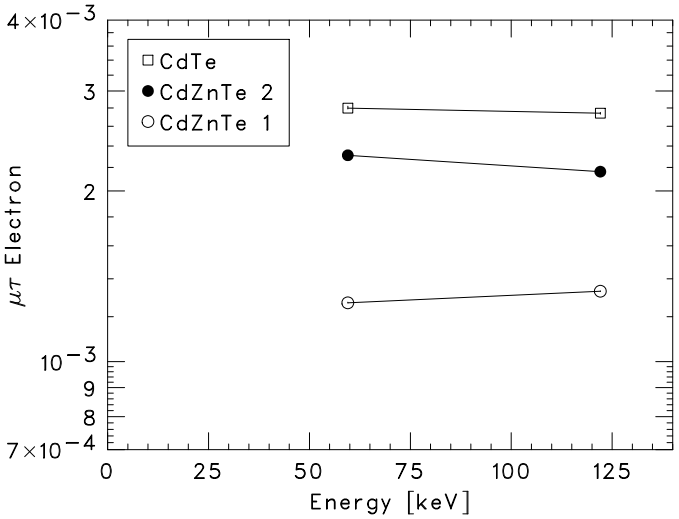


Fig. 12. $(\mu\tau)_{\rm e}$ of CdZnTe/CdTe detectors extracted by spectral fitting method for 59.5 and 122.1 keV $\gamma$-lines.

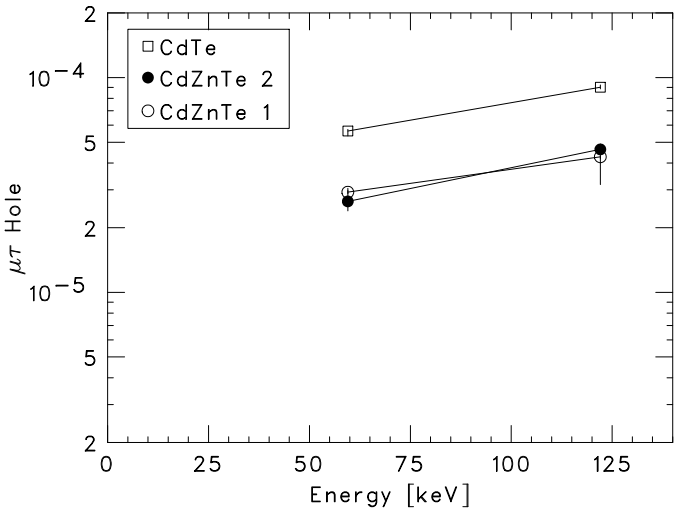


Fig. 13. $(\mu\tau)_{\rm h}$ of CdZnTe/CdTe detectors extracted by spectral fitting method for 59.5 and 122.1 keV $\gamma$-lines.

on the depth from the surface by following Eq.(3).

The simulated spectrum is smoothed by using a Gaussian distribution to model the noise characteristics of the readout electronics, as determined by the spectral fitting parameter $\sigma$ in the "$\mu\tau$-model". The simulated spectra agree well with the actual measurements, as shown in Fig.11. The tail structure is reconstructed almost perfectly by the combination of the charge induction efficiency effect and Compton scattering. The escape peaks are also well reproduced. These results prove that $\mu\tau$ products obtained from the spectral fitting method are reliable and that the "$\mu\tau$-model" works properly.

## IV. Differences in $\mu\tau$ products between detectors

Fig.12 and 13 show the $(\mu\tau)_{\rm e}$ and $(\mu\tau)_{\rm h}$ obtained from 59.5 keV and 122 keV lines for the CdZnTe detector (referred to as CdZnTe 1) used in the previous section. Here, we apply this method to another CdZnTe detector (CdZnTe 2) and also to a THM (Traveling Heator method) CdTe detector we obtained from ACRORAD to investigate the difference of $\mu\tau$ products obtained for different detectors. Each detector has the the same dimensions as CdZnTe 1. Using the two detectors, we obtained spectra by irradiating with $\gamma$-rays of $^{241}$Am and of $^{57}$Co with the same setup as the previous section.

The results obtained from the spectral fitting method are shown in Fig.12 and 13. The $\mu\tau$ products of the three detectors have different values. However, a tendency is found that the high $(\mu\tau)_{\rm h}$ is derived from higher energy line. More studies for this tendency and the differences of $\mu\tau$ products between detectors are now in progress.

## V. Summary and Conclusions

We have developed a "$\mu\tau$-model" spectral fitting method based on basic processes, which can model spectra from CdZnTe/CdTe detectors in a planar configuration. While $(\mu\tau)_e$ is sensitive to the peak channel in a spectrum, $(\mu\tau)_h$ determines the amount of the tail component. By utilizing these phenomena and by fitting $\gamma$-ray spectra taken at least at two different bias voltages, the model provides a new method to extract both $(\mu\tau)_{\rm e}$ and $(\mu\tau)_{\rm h}$ simultaneously. We have applied our method to HPB CdZnTe and THM CdTe detectors and have derived $\mu\tau$ products by properly taking account of Compton scattering and escape peaks. The $\mu\tau$ products were precisely derived from the spectra with small statistical errors of $\sim 1\%$ and $\sim 3\%$ for electrons and holes, respectively. This is because in the method we can directly connect the model histogram with experimental data and can utilize many energy bins for the spectral fitting. The values for 81 and 122 keV lines are consistent with those derived from 59.5 keV line by $\sim 3\%$ and $\sim 20\%$ for electrons and holes, respectively. The tendency that higher $\mu\tau$ values for higher energy lines are still left to be investigated. Monte Carlo simulations using these $\mu\tau$ products reproduce actual spectra almost perfectly. As shown in the comparison with the $\alpha$-particle measurements, the spectral fitting method is a more reliable method to study the characteristics of CdZnTe/CdTe detectors.

## Acknowledgments

This work has been carried out under support of Grant-in-Aid by Ministry of Education, Culture, Sports, Science and Technology of Japan (11440066, 12554006, 13304014). We thank P.G. Edwards for his critical reading of the manuscript and are very grateful for the comments of Ann Parsons and Scott D. Barthelmy (NASA/Goddard Space Flight Center) and the support of eV products, ACRORAD and Clear Pulse.

## References

[1] T. Takahashi and S. Watanabe, "Recent Progress in CdTe and CdZnTe Detector," *IEEE Trans. Nucl. Sci.*, vol. 48, no. 4, pp. 950–959, 2001.

[2] P. Fougeres, P. Siffert, M. Hageali, J.M. Koebel and R. Re-

gal, "CdTe and $Cd_{1-x}Zn_xTe$ for nuclear detectors:facts and fictions," *Nucl. Instr. Meth.*, vol. A 428, pp. 38–44 1999.

[3] Y. Eisen, A. Shor and I.Mardor, "CdTe and CdZnTe gammaray detectors for medical and industrial imaging systems," *Nucl. Instr. Meth.*, vol. A 428, pp. 158–170 1999.

[4] Y. Eisen and Y. Horovitz "Correction of incomplete charge collection in CdTe detectors," *Nucl. Instr. Meth.*, vol. A 353, pp. 60–66 1994.

[5] M. Jung, J. Morel, P. Fougeres, M. Hage-Ali and P. Siffert "A new method for evaluation of transport properties in CdTe and CZT detectors," *Nucl. Instr. Meth.*, vol. A 428, pp. 45–57 1999.

[6] X-Ray Spectral Fitting Package. [Online]. Available: http://heasarc.gsfc.nasa.gov/lheasoft/xanadu/xspec/

[7] S.D. Barthelmy. "The Burst Alert Telescape (BAT) on the Swift MIDEX mission," *Proc. SPIE*, Vol. 4140, pp. 50–63, 2000.

[8] C.M. Stahle, B.H. Parker, A.M. Parsons, L.M. Barbier, S.D. Barthelmy, N.A. Gehrels, D.M. Palmer, S.J. Snodgrass, and J. Tueller. "CdZnTe and CdTe detector arrays for hard X-ray and gamma-ray astronomy," *Nucl. Instr. Meth.*, Vol. A436, pp. 138–145, 1999.

[9] C. Szeles and M. C. Driver, "Growth and properties of semi-insulating CdZnTe for radiation detector applications," *SPIE*, vol. 3446, pp. 2–9, 1998.

[10] K. Hecht, "Zum Mechanismus des lichtelekrischen Primästomes in isolierenden Kristallen", *Zeits. Phys.*, vol. 77, pp. 235, 1932.

[11] A.A. Quaranta, M. Martini and G. Ottaviani, "The pulse shape and the timing problem in solid state detectors," *IEEE Trans. Nucl. Sci.*, vol. 16, no. 2, pp. 35–61, 1969.

[12] Toolkit for the simulation of the passage of particles through matter. [Online]. Available: http://wwwinfo.cern.ch/asd/geant4/geant4.html